Chemical Science

ROYAL SOCIETY OF CHEMISTRY

EDGE ARTICLE

View Article Online
View Journal | View Issue

Cite this: *Chem. Sci.*, 2024, **15**, 13279

All publication charges for this article have been paid for by the Royal Society of Chemistry

Received 20th May 2024
Accepted 16th July 2024

DOI: 10.1039/d4sc03299c

rsc.li/chemical-science

Reversible and size-controlled assembly of reflectin proteins using a charged azobenzene photoswitch†

Cassidy M. Tobin,[a] Reid Gordon,[b] Seren K. Tochikura,[b] Bradley F. Chmelka,[a] Daniel E. Morse[b] and Javier Read de Alaniz *[c]

Disordered proteins often undergo a stimuli-responsive, disorder-to-order transition which facilitates dynamic processes that modulate the physiological activities and material properties of cells, such as strength, chemical composition, and reflectance. It remains challenging to gain rapid and spatiotemporal control over such disorder-to-order transitions, which limits the incorporation of these proteins into novel materials. The reflectin protein is a cationic, disordered protein whose assembly is responsible for dynamic color camouflage in cephalopods. Stimuli-responsive control of reflectin's assembly would enable the design of biophotonic materials with tunable color. Herein, a novel, multivalent azobenzene photoswitch is shown to be an effective and non-invasive strategy for co-assembling with reflectin molecules and reversibly controlling assembly size. Photoisomerization between the *trans* and *cis* (*E* and *Z*) photoisomers promotes or reduces Coulombic interactions, respectively, with reflectin proteins to repeatedly cycle the sizes of the photoswitch-reflectin assemblies between 70 nm and 40 nm. The protein assemblies formed with the *trans* and *cis* isomers show differences in interaction stoichiometry and secondary structure, which indicate that photoisomerization modulates the photoswitch-protein interactions to change assembly size. Our results highlight the utility of photoswitchable interactions to control reflectin assembly and provide a tunable synthetic platform that can be adapted to the structure, assembly, and function of other disordered proteins.

Introduction

As understanding of the sequence–structure–function relationships of proteins grows, researchers have been inspired to incorporate proteins into functional, biomimetic material systems with applications in sensing, therapeutics, and catalysis.[1–5] An exceptional capability of numerous proteins is their stimuli-responsive behavior that facilitates dynamic, out-of-equilibrium processes. This unique feature enables the introduction of diverse functions within biological systems, including on-off modulation of refractive indices, formation of functional strength gradients, and enhancement of biochemical reactions.[6–8] However, platforms that enable rapid and precise control of protein behavior coupled to macroscopic material properties are severely underdeveloped, therefore harnessing the functional properties of proteins in materials remains a significant challenge. Integration of responsive proteins into synthetic systems is expected to enable the advancement of materials with novel properties. Light is a promising stimulus through which control over protein behavior can be attained, due to its high spatiotemporal precision, remote activation, and tunable wavelength and intensity. Longer wavelengths of light (>350 nm) and short pulses of far-UV light have been widely used as a non-toxic, biocompatible stimulus for photopharmacology,[9] drug delivery,[10] and protein-folding applications.[11]

Within biological systems, the on-off behavior of responsive proteins is often controlled by a disorder-to-order transition of intrinsically disordered proteins (IDPs), an inherently stimuli-responsive class of proteins with large fractions of ionic and aromatic amino acids. The high hydrophilicity of IDPs creates sufficient Coulombic repulsion to prevent the collapse of the polypeptide chain into a stable globular or folded structure.[12–15] The disorder-to-order transition can be controlled *in vitro* and *in vivo* by decreasing charge repulsion *via* methods including post-functionalization,[16,17] deprotonation,[18–20] ionic screening,[13,21,22] and co-assembly with an oppositely charged metabolite or biopolymer.[7,23–33] Following charge neutralization, a high valency of associative, non-covalent interactions allows IDPs to form functional, dynamic assemblies that regulate enzymatic

[a]*Department of Chemical Engineering, University of California, Santa Barbara, California 93106, USA*

[b]*Department of Molecular, Cellular, and Developmental Biology, University of California, Santa Barbara, California 93106, USA*

[c]*Department of Chemistry and Biochemistry, University of California, Santa Barbara, California 93106, USA. E-mail: javier@chem.ucsb.edu*

† Electronic supplementary information (ESI) available: Synthetic procedures and characterization, reflectin protein purification and methods for sample preparation, additional characterization of protein-photoswitch complexes. See DOI: https://doi.org/10.1039/d4sc03299c

activity, biomolecule sequestration, and cell properties (Fig. 1A). By encoding light-responsive control over the transient interactions that assemble IDPs, we can begin to leverage their novel functions to develop materials with programmable properties.

Reflectin proteins are a class of IDPs isolated from squid species that are responsible for the dynamic and tunable structural color allowing squid to camouflage and communicate with their environment.[8,34] The reflectin A1 wildtype protein (hereafter referred to as reflectin) is a cationic IDP whose intrinsic disorder derives from a large fraction of histidine and arginine amino acids that are localized in positively charged blocks. As a result, reflectin cannot initially form stable secondary structures and instead exists in a random coil conformation (Fig. 1A).[35] Charge neutralization of the cationic blocks reduces Coulombic repulsions that preserve the monomeric unassembled state of reflectin so that attractive interactions become dominant, resulting in the condensation, folding, and assembly of reflectin into large complexes.[35] *In vivo*, neurotransmitter-triggered phosphorylation drives assembly by reducing the net charge of reflectin. *In vitro*, assembly of reflectin can be manipulated by using protein mutation,[35] ionic screening,[21] deprotonation,[18] and electrochemical reduction,[36,37] which act as surrogates for phosphorylation by neutralizing or screening charges. There is significant interest in developing reflectin-mediated biophotonic materials[38–43] and critical to this goal is the development of novel light-responsive strategies to reversibly control the assembly of disordered proteins like reflectin.

Reversible control of protein function has been achieved by integration of photoswitchable molecules, such as azobenzenes,[44–50] that undergo a change in conformation upon irradiation which, subsequently, modulates protein or peptide properties, such as conformation,[51–56] enzymatic activity,[57–60] and ligand binding.[61–64] For photocontrol of peptide systems, azobenzenes are frequently covalently linked in the peptide backbone or side chain, which allows their photoisomerization to impart local control of protein dynamics.[65] However, the photo-controlled assembly of reflectin and other IDPs requires a photoswitch that can interact with protein side chains more generally to affect protein–protein interactions and assembly. Photoresponsive capture of proteins has been achieved in supramolecular systems with a high valency of electrostatic interactions,[66–69] but photoswitchable assembly has only been applied to highly charged biopolymers, such as double-stranded DNA[70] and polysaccharides.[71,72] To the best of our knowledge, suitable photoswitches to reversibly assemble systems as complicated as disordered proteins have not yet been developed.

Here, we report a photoswitchable molecule that can reversibly tune the mean dimension of reflectin protein complexes *via* electrostatic co-assembly. We studied the assembly behavior of reflectin proteins with multivalent molecules to inform our design of an azobenzene photoswitch that can reversibly control this behavior. We demonstrated that, upon irradiation with different wavelengths of light, azobenzene photoisomerization alters the efficacy of its electrostatic crosslinking behavior between the cationic blocks on

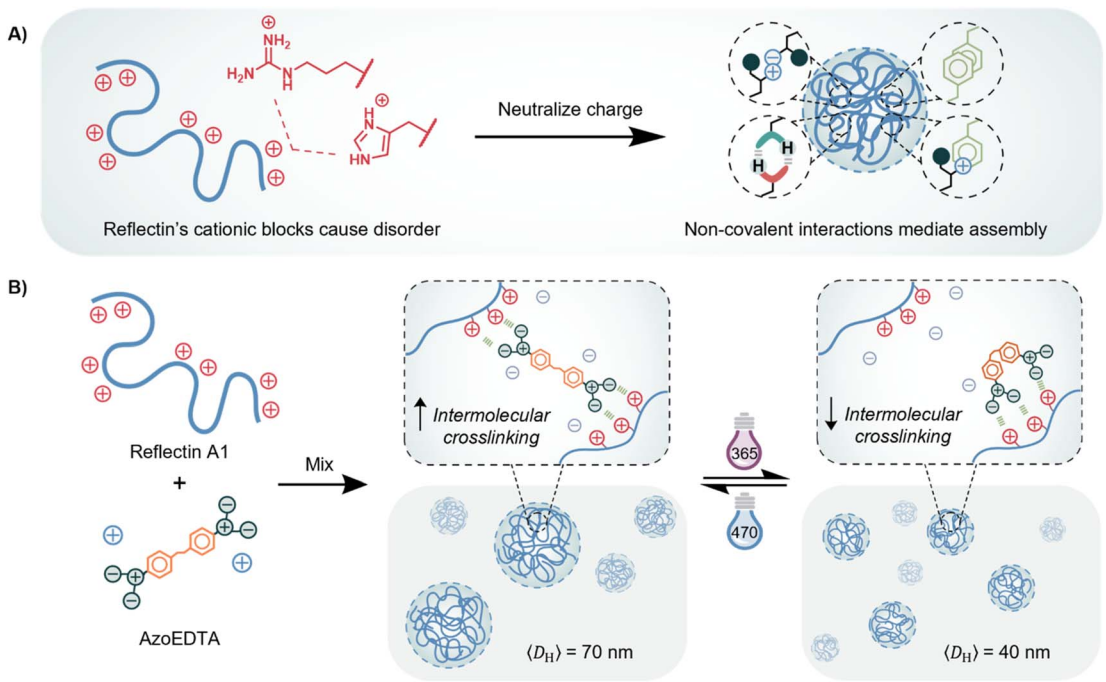

Fig. 1 A) Reflectin A1 wildtype protein has alternating, positively charged regions whose Coulombic repulsions initially prevent condensation, folding and formation of higher ordered structures. Charge neutralization overcomes these repulsive interactions, driving associative, non-covalent interactions that form large complexes of reflectin proteins. Counterions on reflectin protein not shown for simplicity. (B) Schematic diagram of photo-controlled electrostatic interactions between reflectin proteins and multivalent azobenzene photoswitches with anionic end groups.

reflectin, allowing the reflectin-photoswitch assemblies to be controlled between 2 discrete mean sizes under the optimized conditions (Fig. 1B). To our knowledge, this is the first demonstration of photoswitchable and cyclable control of assembly size of a disordered protein. We expect the results of this work to be generally applicable for other cationic IDPs and to inform design requirements for future light-responsive IDP systems.

Results and discussion

Molecular design, synthesis, and characterization of photoresponsive crosslinker

The first objective was to design a photoswitch that could reversibly modulate electrostatic crosslinking of reflectin proteins in aqueous environments. Prior studies of reflectin have not used multivalent molecules to induce assembly and the design rules for such a switch were unknown. For globular proteins and disordered proteins, co-assembly behavior with multivalent small molecules is typically influenced by the number and type (*e.g.*, ionic *versus* aromatic) of interaction sites.[23,24,26,33] Reflectin is a 43 kDa protein with a net charge ≥ +52 in its disordered state (Fig. S1†).[35] Multivalent (and not light-responsive) carboxylic acids were screened with cationic reflectin to determine the number of anionic moieties required to drive electrostatically-mediated assembly with reflectin. Carboxylic acids form strong but dynamic electrostatic interactions with histidine and arginine amino acids, which, we hypothesized, will allow a multivalent photoswitch to have rearrangeable interactions with the protein.[73,74] To ensure all acids were deprotonated, stock solutions of the small molecules were prepared in a 10 mM MOPS buffer at pH 7.50. At this pH, histidine side chains are deprotonated and reflectin is partially assembled with a net charge of +17. Therefore, the multivalent acids were expected to interact with arginine side chains. It is noted that thermodynamics of assembly related to buffering species were not explored in this study.

The sizes of the protein assemblies formed were measured with dynamic light scattering (DLS), where an increase in hydrodynamic diameter (D_H) indicated assembly. As shown in Fig. 2A, for 200 μM of a small molecule acid and 20 μM of reflectin, small molecules with more than 2 acid groups, ethylenediaminetetraacetic acid (**3**, EDTA) and pentetic acid (**4**), are needed to form larger reflectin assemblies relative to the control (0). Dicarboxylic acids, succinic acid (**1**) and suberic acid (**2**), are not able to induce assembly at concentrations up to 400 μM (Fig. S2†), which is consistent with literature findings that ≥3 interactions are necessary to promote electrostatically-mediated assembly,[26] as corroborated by Fig. 2A which also shows that at least 3 acid groups are needed for assembly.

Therefore, we hypothesized that multivalent molecular photoswitches with higher numbers of anionic charges would promote assembly of reflectin from its initially disordered state. Under weakly acidic conditions, reflectin is disordered with a net charge of +52. Taking EDTA as a suitable model, Fig. S3† shows that 5 times more EDTA is needed to form reflectin assemblies at pH 4.50 than at pH 7.50. The assembly behavior between EDTA and reflectin changes under acidic conditions, due to reflectin's random coil structure, its higher charge density, and the decreased valency of EDTA to (−2) following amine protonation. The co-assembly between positively charged reflectin and multianionic molecules like EDTA occurs *via* ion-bridging of individual cationic proteins (under acidic conditions) or ion-bridging of positively charged protein assemblies (under neutral to basic conditions), rather than electrostatic screening (Fig. S4†).

Based on our multivalent small molecule studies, we next sought to achieve photoresponsive reflectin assembly by using an EDTA-inspired azobenzene photoswitch functionalized with two bidentate acid ligands. Upon photoisomerization, the *cis* isomer becomes more polar, nonplanar, and conformationally compact compared to the *trans* isomer.[47] This conformation change limits the range of electrostatic interactions that the *cis* isomer can have with reflectin and is expected to favor electrostatic interactions with a single reflectin protein, rather than the formation intermolecular, electrostatic crosslinks between multiple proteins. Therefore, we hypothesized that the *cis* isomer would form smaller photoswitch-protein complexes compared to the *trans* isomer.

The multianionic, water-soluble azobenzene photoswitch was prepared by coupling a dicarboxylic acid azobenzene with a protected acid ligand (Fig. 2B). The protecting ester groups were removed by saponification with sodium hydroxide to yield the desired azobenzene photoswitch (**azoEDTA**) in a convergent, 66%-yield synthesis. Full experimental procedures and characterization are described in the ESI.† The high-yield synthesis provides a platform that can facilitate tunability of photoswitch structure. For example, *ortho*-substitution of the azobenzene core would create a visible light-responsive photoswitching system,[48] and *N*-alkylation of Boc-ethylenediamine with other protected acids or bases can tune the multivalent functionality.

To characterize the switching properties of **azoEDTA** under conditions relevant to our reflectin system, a 20 mM sodium acetate buffer at pH 4.50 was used. The *trans–cis* notation is hereafter used to distinguish between the (*E*)- and (*Z*)-azoEDTA photoisomers. Titration of *trans*-azoEDTA with hydrochloric acid confirmed that **azoEDTA**'s carboxylate groups are completely deprotonated at pH > 4 (Fig. S5†). At pH 4.50, **azoEDTA** is therefore fully ionized, as shown in Fig. 2C, and will undergo reversible photoisomerization with 365 nm and 470 nm light. The UV-visible (UV-vis) spectra and further optical characterization of **azoEDTA** are shown in Fig. 2D and S6.† At the 365 nm photostationary state (PSS_{365}), 30% conversion to *cis*-azoEDTA was reached. Upon irradiation with 470 nm light, PSS_{470} was composed of 91% *trans*-azoEDTA (Fig. S7†). Low conversion of the *trans* → *cis* photoisomerization in polar solvents is consistent with literature findings.[53,56,71] The *cis* isomer exhibited excellent thermal stability, with a half-life of 9.9 days under ambient conditions (Fig. S8†).

The photoisomerization kinetics of **azoEDTA** under 365 nm and 470 nm light irradiation were studied using time-dependent UV-vis spectroscopy. The photoisomerization reaction of **azoEDTA** follows first-order rate kinetics in both directions, and the *trans* → *cis* rate coefficient, $k_{A,365} = 8.59 \times$

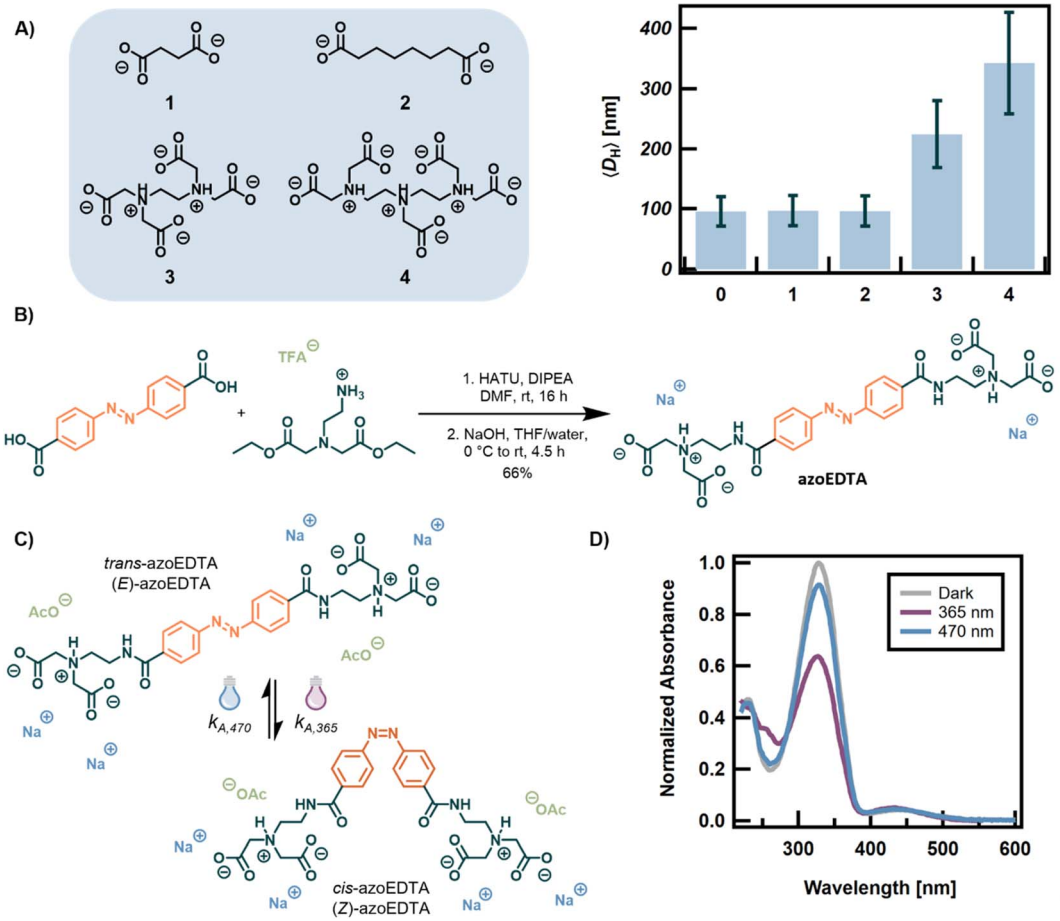

Fig. 2 (A) Carboxylic acids with varying structure and number of acid groups, but constant valency, were studied for their effects on assembly (counterions not shown for simplicity). The mean hydrodynamic diameters ($\langle D_H \rangle$) of reflectin assemblies prepared as 50 μL samples were measured with DLS. A 20 μM reflectin solution, identically buffered but with no multivalent acid (0), was used as the control. (B) Synthetic scheme for convergent synthesis of **azoEDTA** with 66% yield. (C) Photoreversible *trans–cis* (*E–Z*) isomerization of **azoEDTA** under weakly acidic conditions. (D) Absorption spectra for 350 μM **azoEDTA** in 20 mM sodium acetate buffer (pH 4.50) at the photostationary states for 365 nm and 470 nm light.

10^{-3} min^{-1}, is an order of magnitude slower than the *cis* → *trans* rate coefficient, $k_{A,470} = 9.10 \times 10^{-2}$ min^{-1} (Fig. S9 and Table S1†). A faster *cis* → *trans* isomerization is consistent with literature findings for photoswitching of *para*-substituted azobenzenes in polar solvents and is attributed to a rotational isomerization mechanism about the azo bond.[47,75,76] As expected, **azoEDTA** can undergo at least 5 irradiation cycles with no detectable fatigue.

Co-assembly of *trans*- and *cis*-azoEDTA with reflectin protein

After synthesis of the **azoEDTA** photoswitch, the co-assembly behavior of **azoEDTA** with reflectin was investigated to determine a suitable concentration regime for the photoswitching behavior. Unless otherwise stated, a 20 mM sodium acetate buffer at pH 4.50 was used for protein dialysis and sample preparation. A concentrated stock solution of *trans*-azoEDTA (2.2 mg mL^{-1}, 3.7 mM) was diluted into the buffer to obtain 16–920 μM photoswitch. **AzoEDTA** does not self-assemble or aggregate at the concentrations studied. Dialyzed reflectin was added to the solution from a concentrated stock (~9 mg mL^{-1}) to reach a concentration of 8 μM of protein. For all studies shown, **azoEDTA**–reflectin samples were given 120 min to equilibrate in the dark (Fig. S10 and S11†). The protein assemblies formed were characterized by turbidity, size, and structure (Fig. 3A). Once prepared, assembly between the **azoEDTA** and reflectin proteins was driven by Brownian motion of the solutes, enthalpic interactions between the oppositely charged molecules, and favorable entropic release of counterions *via* complexation.[13] Due to the random nature of this process, relatively large dispersities in size were expected.

The concentration of *trans*-azoEDTA was varied to study its effect on the properties of the protein complexes formed. The turbidity and size were measured by UV-vis spectroscopy and DLS, respectively, to determine the minimum concentration of *trans*-azoEDTA for protein assembly formation. Monomeric, unassembled reflectin was measured to have 5% turbidity and a mean hydrodynamic diameter ($\langle D_H \rangle$) of 8.9 ± 3 nm. For higher concentrations of *trans*-azoEDTA, the samples became visually more turbid. Turbidity was shown to increase for

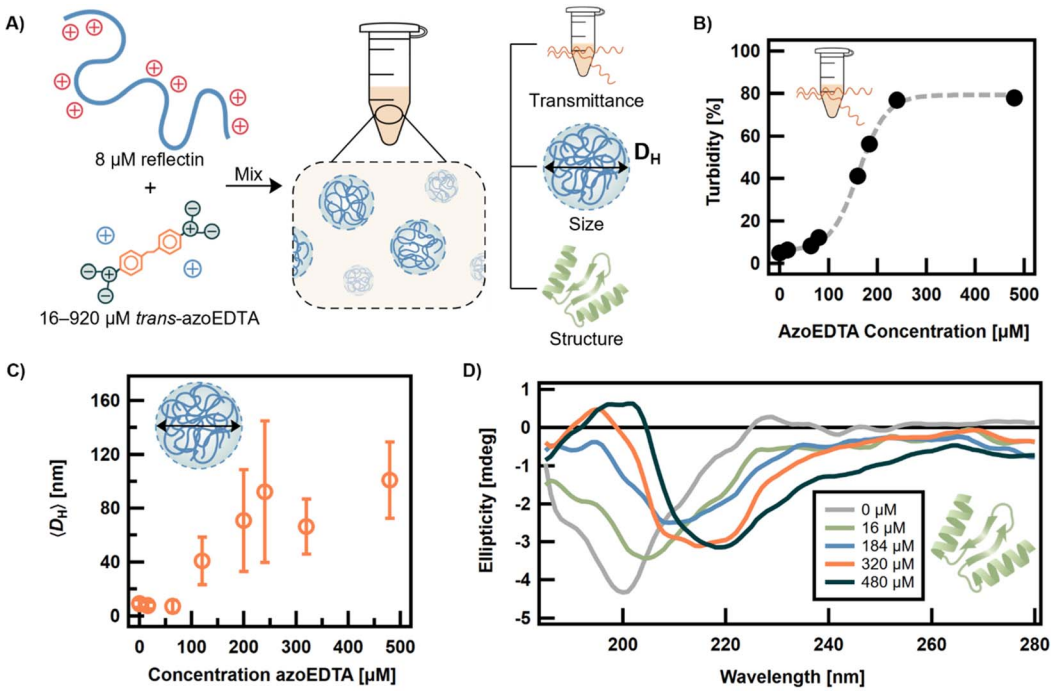

Fig. 3 A) Schematic diagram of sample preparation and characterization of assembly of *trans*-azoEDTA–reflectin protein complexes. Counterions on reflectin protein not shown for simplicity. For a fixed reflectin concentration of 8 μM, the concentration of *trans*-azoEDTA was varied over the range of 16–920 μM. All samples were prepared in a 20 mM sodium acetate buffer (pH 4.50). (B) Turbidity of the *trans*-azoEDTA–reflectin system was measured at 400 nm (black dots) and modelled with a sigmoidal function (gray line). (C) The mean hydrodynamic diameter (⟨D_H⟩) of samples measured by DLS. The ⟨D_H⟩ of monomeric, disordered reflectin is 8.9 ± 2.8 nm. Error bars represent standard deviations of average diameter. (D) Ellipticity of **azoEDTA**–reflectin complexes measured by CD.

concentrations of *trans*-azoEDTA > 100 μM and follows a sigmoidal model (Fig. 3B). The trend in turbidity is consistent with the evolution in size of the assemblies measured by DLS (Fig. 3C). At 120 μM *trans*-azoEDTA, ⟨D_H⟩ was 40.8 ± 18 nm, indicating the formation of **azoEDTA**–reflectin complexes. This large change in ⟨D_H⟩ indicates that multiple reflectin proteins are associated with multiple **azoEDTA** molecules during assembly. The minimum concentration of *trans*-azoEDTA required for measurable assembly (>100 μM) is an order of magnitude lower than the concentration of EDTA required for assembly under the same conditions (Fig. S12†). We attribute this behavior to the larger molecular size and planar aromatic core of *trans*-azoEDTA, relative to EDTA, which allow the photoswitch to more effectively form intermolecular, electrostatic bridges between reflectin molecules *via* electrostatic and weak hydrophobic interactions. For concentrations of *trans*-azoEDTA below 480 μM, ⟨D_H⟩ is not sensitive to *trans*-azoEDTA concentration and assembly is controlled to sizes between 40–100 nm. Interestingly, at concentrations greater than 480 μM, ⟨D_H⟩ is linearly related to concentration of **azoEDTA** (Fig. S13†). We hypothesize that at concentrations of *trans*-azoEDTA ≥ 480 μM, free reflectin becomes sufficiently dilute such that, rather than electrostatically crosslinking reflectin molecules, excess **azoEDTA** acts as a crosslinker between existing protein-photoswitch assemblies.

To study the effect of *trans*-azoEDTA concentration on the secondary structure of **azoEDTA**–reflectin assemblies, circular dichroism (CD) spectroscopy was used. Of note, **azoEDTA** did not show chirality in the absence of reflectin (Fig. S14†). Monomeric reflectin with no **azoEDTA** in solution has a disordered, random coil conformation, shown by a minimum in ellipticity at 200 nm (Fig. 3D).[35] As the concentration of **azoEDTA** was increased, the ellipticity minima shifted toward longer wavelengths, indicating that significant structural changes in the reflectin proteins occur during assembly of the protein-photoswitch complexes. Thus, as the concentration of **azoEDTA** increases and the photoswitch interacts with reflectin to form protein assemblies, the charge repulsion that causes reflectin's disordered state is reduced, allowing reflectin to fold and form α helix (ellipticity minima at 208 nm and 217 nm) and β sheet (broad ellipticity minimum centered at 220 nm) structures, even for concentrations below 120 μM. This behavior is consistent with previous secondary structural studies of reflectin assemblies which show the presence of α helix and β sheet structures.[35,77] However, at concentrations >480 μM, only β sheet character is observed which indicates aggregation behavior that is incompatible with a photoresponsive system.[78,79] Interestingly, EDTA–reflectin assemblies follow the same evolution of ellipticity as the **azoEDTA**–reflectin system, but sodium chloride–reflectin assemblies show ellipticity minima indicating both α helix and β sheet features at high concentrations of salt (Fig. S15†). We propose that co-assembly with multivalent molecules follows a different assembly mechanism than ionic screening which causes reflectin to form more

β sheet structures at high concentrations of the oppositely charged molecule.

As discussed, we hypothesized that *cis*-azoEDTA isomer would have a reduced propensity to form intermolecular, electrostatic bridges between reflectin proteins, thus decreasing the assembly size of the protein complexes formed. The assembly size and interaction stoichiometry of the *trans* and *cis* isomers were compared at the thermally-relaxed and at the 365 nm photostationary states (Fig. 4A). **AzoEDTA**–reflectin samples with *cis*-azoEDTA were prepared as previously described, but the photoswitch stock solution was irradiated for 30 min with 365 nm light prior to sample preparation. Due to the long half-life of *cis*-azoEDTA, thermal relaxation was not a concern on the timescale of the experiments described.

The co-assembly behaviors of *trans*-azoEDTA and *cis*-azoEDTA with reflectin were evaluated by comparing the assembly sizes formed from the two photoisomers. For 240 μM **azoEDTA** and 8 μM reflectin, Fig. 4B shows that an assembly size of 91 ± 39 nm was measured for assemblies with *trans*-azoEDTA and an assembly size of 60 ± 37 nm was measured for assemblies with *cis*-azoEDTA. This 33% smaller diameter of *cis*-azoEDTA–reflectin assemblies supports our hypothesis that the *cis* isomer forms smaller assemblies, because its compact conformation hinders its ability to form electrostatic, intermolecular bridges between reflectin proteins compared to the *trans* isomer.

The interaction stoichiometry of **azoEDTA** with reflectin in the protein assemblies was estimated using protein precipitation experiments. Centrifugation of **azoEDTA**–reflectin samples precipitated the protein assemblies into an orange pellet with a transparent supernatant solution (Fig. S16†). The supernatant did not contain any measurable **azoEDTA**–reflectin assemblies *via* DLS. Neither the photoswitch nor reflectin precipitated in control experiments (Fig. S17†). The concentrations of **azoEDTA** and reflectin in the supernatant were used to estimate, by difference, the concentration of each species in the dense assembled phase from which the interaction stoichiometry was calculated between **azoEDTA** and reflectin (Fig. S18†). Detailed experimental procedures can be found in the ESI.† For concentrations of *trans*-azoEDTA that assemble with reflectin (>100 μM), the interaction stoichiometry is constant for both photoisomers and the percentage of non-interacting **azoEDTA** increases linearly (Fig. 4C and S19†). This behavior is consistent with the controlled assembly for concentrations of *trans*-azoEDTA <480 μM, as previously discussed. Under these conditions, 18 ± 1 and 11 ± 2 molecules of *trans*- and *cis*-azoEDTA, respectively, interact per reflectin protein to form protein complexes. Since the 4 carboxylate groups of a *cis*-azoEDTA molecule are more likely to interact with a single reflectin protein, it is reasonable that the observed ratio of *cis*-azoEDTA to reflectin is lower than the *trans*-azoEDTA to reflectin ratio. Fig. 4D shows that the fraction of free reflectin in the

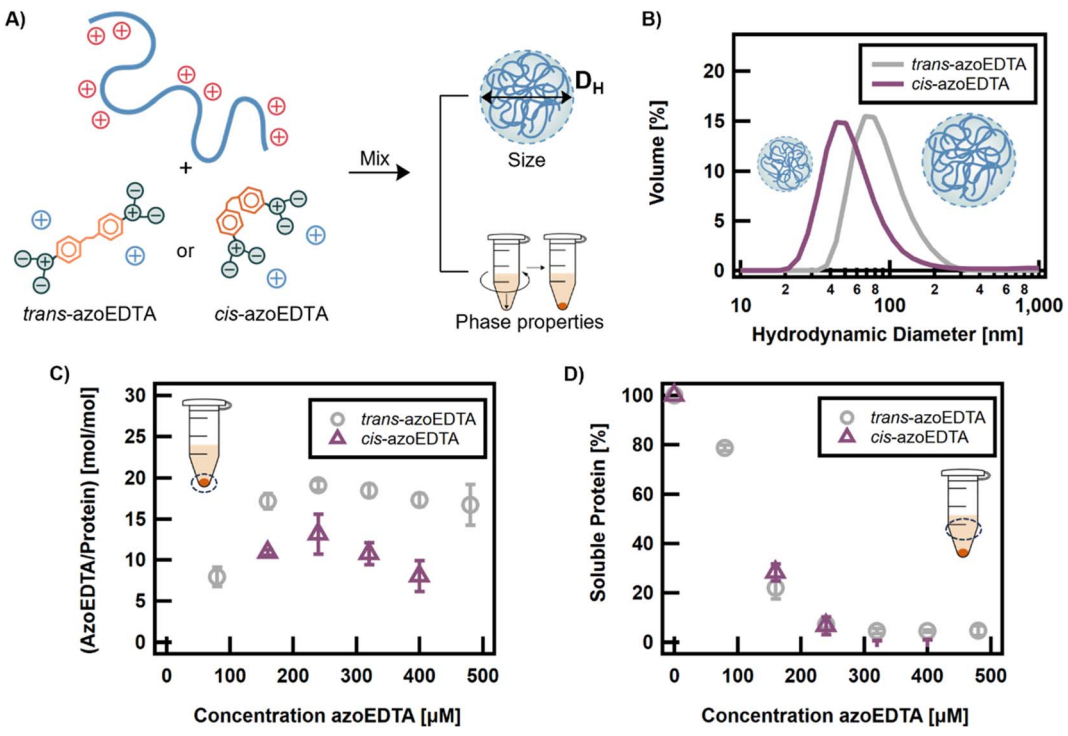

Fig. 4 A) Schematic of sample preparation and characterization of assembly of **azoEDTA**–reflectin protein complexes for *trans*-azoEDTA or *cis*-azoEDTA. For a fixed reflectin concentration of 8 μM, the concentration of *trans*- and *cis*-azoEDTA was varied over the range of 80–480 μM. (B) DLS shows change in particle size distribution for **azoEDTA**–reflectin assemblies with 240 μM **azoEDTA**. (C) Ratio of moles of **azoEDTA** to moles of reflectin in the precipitable, assembled protein phase. Error bars represent the standard deviation calculated from 3 independent experiments. (D) Percent of soluble protein remaining in supernatant after centrifugation. Error bars represent the standard deviation calculated from 3 independent experiments.

supernatant does not depend on the photoisomer of **azoEDTA**. Taken together, Fig. 4C and D indicate that *trans–cis* photoisomerization decreases the number of protein-photoswitch interactions but does not affect the amount of interacting reflectin. Thus, for a given photoswitch concentration, *cis*-azoEDTA forms less electrostatic interactions with reflectin and neutralizes less of the positive charge from the reflectin proteins than the *trans* isomer, which results in the formation of smaller reflectin assemblies.

To optimize the photoswitchable control of assembly size, it is crucial to minimize behaviors that lead to uncontrolled, nonspecific aggregation. Our study of the co-assembly of *trans*- and *cis*-azoEDTA with reflectin has revealed that concentrations of **azoEDTA** < 320 μM minimize assembly formations with $\langle D_H \rangle$ > 100 nm, β sheet formation, and the presence of non-interacting **azoEDTA**, each of which could make the system prone to aggregation.

Photoresponsive sizes of azoEDTA–reflectin assemblies

Based on the above results, the co-assembly of **azoEDTA** with reflectin was monitored following *in situ* light irradiation using samples prepared with 240 μM of the **azoEDTA** photoswitch and 8 μM reflectin. In the absence of **azoEDTA**, reflectin assemblies do not change in size or structure following light irradiation (Fig. S20†). The absorbance and photoswitching behavior of the system was studied using time-dependent UV-vis spectroscopy. Compared to the light absorbance spectrum of **azoEDTA**, the maximum absorption wavelength of the **azoEDTA**–reflectin system showed a hypochromic and bathochromic shift to 338 nm (Fig. S21†). The red shift in absorbance is attributed to a more hydrophobic environment for *trans*-azoEDTA resulting from interactions with reflectin and indicates localization of the photoswitches in the interiors of the assemblies. This behavior is consistent with previous observations for protein-binding chromophores.[57,80,81] The absorbance spectrum also shows light-responsive turbidity that is consistent with the different sizes of the protein-photoswitch complexes at each PSS (Fig. S22†).

Therefore, we propose to model the absorbance photoresponse by accounting for two processes that occur on separate timescales: the fast, reversible photoisomerization of **azoEDTA** ($k_{A,365}$ and $k_{A,470}$) and the associated, slow assembly-disassembly of reflectin-photoswitch complexes ($k_{R,365}$ and $k_{R,470}$) (Fig. 5A). The kinetics of **azoEDTA** photoswitching and assembly were assessed by fitting the time-dependent UV-vis data (Fig. 5B) to a biexponential model, where assembly-disassembly of the **azoEDTA**–reflectin complexes was assumed to be a pseudo-first order process. A detailed explanation of the photoresponsive absorbance model can be found in the ESI.† When the sample was first irradiated with 365 nm light, $k_{A,365}$ was 50% faster in the presence of reflectin than for a solution without reflectin. For all other irradiation cycles, $k_{A,365}$ and $k_{A,470}$ (Table S2†) were determined to be the same order of magnitude as observed for the **azoEDTA**-only solution (Table S1†). Compared to the rates of isomerization, the $k_{R,365}$ was approximately 70 times slower than $k_{A,365}$, and $k_{R,470}$ was approximately 100 times slower than $k_{A,470}$. Such slow rates of assembly-disassembly are consistent with the slow diffusion of **azoEDTA**–reflectin complexes and free reflectin molecules (Table S3†), relative to the diffusion of free *trans*- and *cis*-azoEDTA in solution.[82,83] The assembly-disassembly of the reflectin–**azoEDTA** complexes also continued to occur even in the absence of light, meaning that once **azoEDTA** photoisomerization has reached equilibrium, light irradiation is not required to assemble or disassemble the **azoEDTA**–reflectin complexes. In addition, the experimental data show that the photoswitching of the **azoEDTA**–reflectin system is reversible and does not deteriorate over three cycles. Taken together, these results indicate that sufficient time after irradiation is necessary for a significant change in assembly size to be detected.

The change in assembly size following UV- or blue-light irradiation of the **azoEDTA**–reflectin assemblies was monitored by DLS. Prior to sample irradiation, the mean size of the photoswitch-protein assemblies was measured to be 74 ± 52 nm. As shown in Fig. 5C, after *in situ* UV light irradiation (365 nm), the size of the protein-photoswitch complexes was measured to be 39 ± 25 nm, or 53% of the initial mean assembly size. These results are consistent with the mean sizes measured in the co-assembly studies. After irradiation of the same sample with blue light (470 nm), the mean protein-photoswitch assembly size increased to 55 ± 52 nm, or 80% of the initial assembly size. Statistical analysis with paired sample *t*-tests showed that the changes in mean diameter following light irradiation are statistically significant ($p < 0.05$). The PSS_{470} was 91% *trans*-azoEDTA, as established by ^{1}H NMR, which explains the incomplete recovery of D_H with blue light. When sufficient time (>10 min) is allowed for the protein-photoswitch complexes to assemble or disassemble, two cycles of photocontrolled $\langle D_H \rangle$ were measured by DLS with no decay in magnitude of assembly size change (Fig. 5D and S23†). The remnant population of *cis*-azoEDTA at the PSS_{470} limits the recovery of the initial **azoEDTA**–reflectin assembly size. By initiating irradiation cycles at PSS_{365}, a consistent magnitude of size change can be achieved over two cycles (Fig. S24†). After two irradiation cycles, no significant change in $\langle D_H \rangle$ was measured by DLS. The derived count rates from the DLS measurements also cycle with UV- and blue-light irradiation (Fig. S25 and 26†), indicating that particles did not settle out of solution or aggregate during irradiation or measurement.

Circular dichroism analyses show that the secondary structures of **azoEDTA**–reflectin complexes also exhibit cyclable behavior upon light irradiation. As shown above, at higher concentrations of **azoEDTA** in solution with reflectin, more α helix and β sheet (*i.e.*, more ordered) features are observed. Therefore, if the interaction stoichiometry decreases for *cis*-azoEDTA at PSS_{365}, we expect the system to show less order. Fig. 5E shows how ellipticity, and therefore the structural features of the reflectin–**azoEDTA** assemblies, changes with *in situ* photoisomerization of **azoEDTA**. Prior to light irradiation, the reflectin–**azoEDTA** complexes show α helix and β sheet characteristics and a minimum in ellipticity at 206 nm. With 365 nm light irradiation, the ellipticity minimum shifts to 203 nm and its magnitude increases, indicating that the

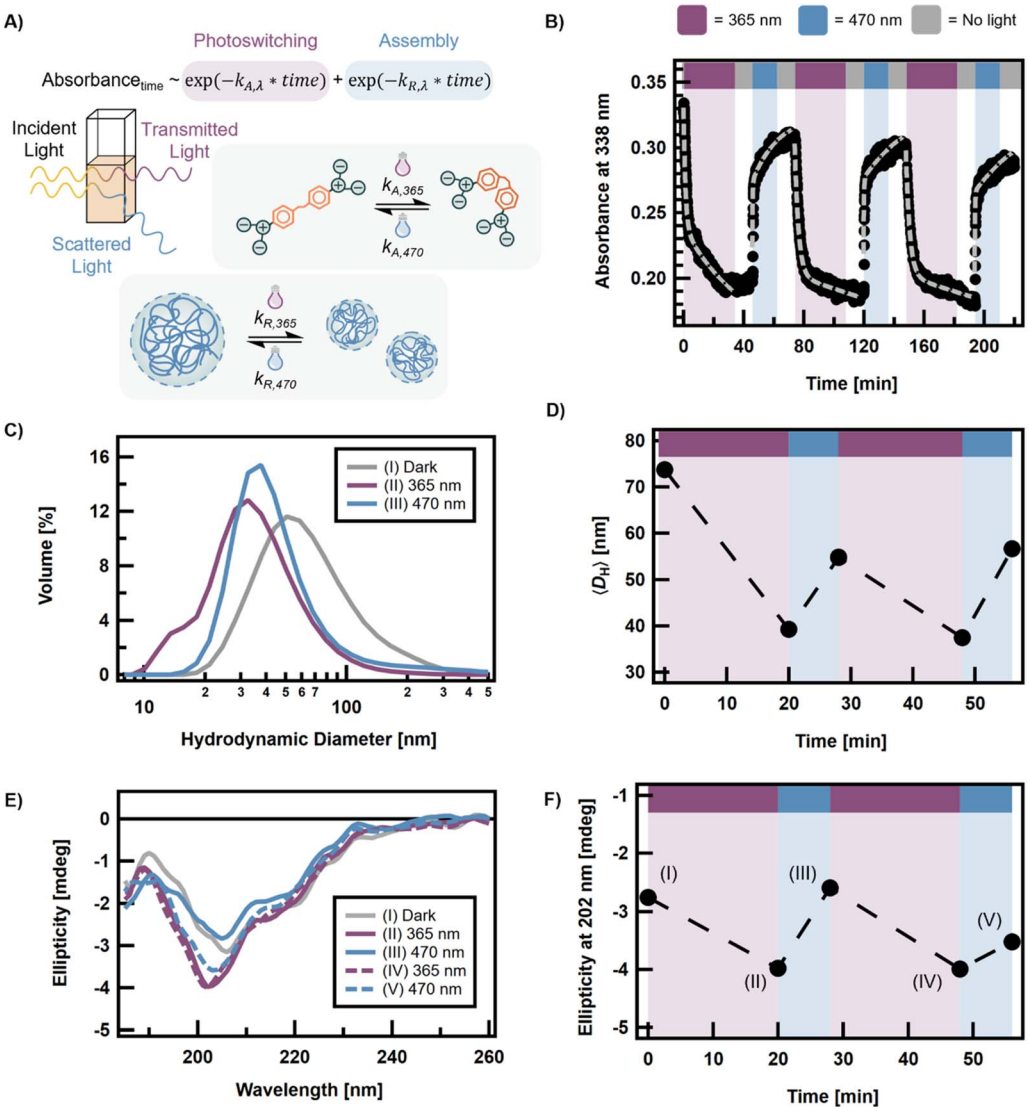

Fig. 5 Photoresponse of the **azoEDTA**–reflectin system for 8 μM reflectin and 240 μM **azoEDTA**. (A) Schematic illustrating how photoisomerization and turbidity contribute to changes in the measured absorbance of the system upon irradiation. (B) Time-dependent absorbance was collected for 3 cycles with UV light irradiation for 34 min, blue light for 17 min, and no light for 12 min following each irradiation (black dots). The behavior can be fit to a biexponential model (gray lines) that accounts for the photoisomerization and assembly processes. Rate coefficients are given in Table S2.† (C) DLS shows a change in assembly size distribution after irradiation with UV and blue light. (D) The change in $\langle D_H \rangle$, as measured by DLS, can be cycled twice. (E) Evolution of ellipticity of dark-equilibrated **azoEDTA**–reflectin complexes (I) when exposed to 365 nm (II, IV) and 470 nm (III, V) irradiation. (F) Ellipticity at 202 nm can be cycled as a function of light irradiation.

assemblies are becoming less ordered. The initial ellipticity spectrum can be recovered with 470 nm light irradiation, showing that the photoinduced structural changes are reversible. When the ellipticity at a single wavelength is shown as a function of irradiation time, as shown in Fig. 5F, it is evident that ellipticity is cyclable over two irradiation cycles. This finding indicates that, similarly to the change in $\langle D_H \rangle$, the protein-photoswitch assemblies have structural features that are cyclable. However, incomplete recovery of structure is observed after the second cycle, potentially due to irreversible binding of **azoEDTA** with reflectin. To improve the cyclability of the **azoEDTA**–reflectin system, we hypothesize that heteroatom substitution of the azobenzene moiety will reduce hydrophobic interactions between the photoswitch and protein that might lead to irreversible binding and uncontrolled, nonspecific aggregation.

Conclusions

In this study, the screening of the electrostatic interactions of reflectin proteins by co-assembly with a multivalent azobenzene photoswitch (**azoEDTA**) is shown to be a tool for controlling the formation and size of reflectin-photoswitch assemblies. Following a robust photoswitch synthesis that is easily adaptable for other charged biopolymers, we characterized the assembly behavior of **azoEDTA** with reflectin under weakly

acidic conditions and identified 120–320 μM **azoEDTA** as the ideal concentration regime for controlled assembly of protein-photoswitch complexes with minimal evidence of nonspecific aggregation. We showed that the interaction stoichiometry between *cis*-azoEDTA and reflectin is 40% lower than with the *trans* isomer, indicating that *cis*-azoEDTA forms less electrostatic interactions with the protein and thus forms smaller protein assemblies. Finally, we demonstrated the utility of **azoEDTA** to produce photoresponsive and cyclable changes in the size and secondary structure of reflectin–**azoEDTA** assemblies with *in situ* light irradiation. Under 20 min of UV-light irradiation and 8 min blue-light irradiation, the mean diameter of the protein assemblies was shown to cycle between 74 ± 52 nm and 39 ± 25 nm. To the best of our knowledge, this is the first report of the co-assembly of a high-molecular-weight, cationic, disordered protein with an oppositely charged photoswitch and the photoresponsive control of protein assembly size. The transient nature of electrostatic interactions and the relatively non-selective character of the carboxylate moiety is expected to enable similar charged molecules to be used for the photoresponsive assembly of other oppositely charged proteins. Furthermore, this approach is attractive as a general tool for the formation of photoresponsive complexes of disordered proteins, which are currently finding promising applications in materials, biocatalysis, and therapeutics.

Data availability

The datasets supporting this article have been uploaded as part of the ESI.†

Author contributions

C. M. T. and J. R. d. A. conceptualized the project. C. M. T. conducted the experiments with supervision from J. R. d. A. R. G. and S. K. T. provided reflectin protein and methodology input. The manuscript was written by C. M. T. All authors reviewed and edited the manuscript.

Conflicts of interest

There are no conflicts to declare.

Acknowledgements

The authors thank Yahya Al Sabeh, Justin Paluba, and Brandon Malady for their assistance on reflectin synthesis and Lior Sepunaru for instrument access. This research was sponsored by the U.S. Army Research Office and accomplished under cooperative agreement W911NF-19-2-0026 and contract W911NF-19-D-0001 for the Institute for Collaborative Biotechnologies. The content of the information does not necessarily reflect the position or the policy of the Government, and no official endorsement should be inferred. This work utilized NMR instruments supported by the National Science Foundation under award No. MRI-1920299. This work made use of the MRL Shared Experimental Facilities that are supported by the MRSEC Program of the NSF under Award No. DMR 2308708; the UC Santa Barbara MRSEC is a member of the Materials Research Facilities Network (**https://www.mrfn.org**).

References

1 R. Zeng, C. Lv, C. Wang and G. Zhao, *Biotechnol. Adv.*, 2021, **52**, 107835.
2 S. Pradhan, A. K. Brooks and V. K. Yadavalli, *Mater. Today Bio*, 2020, **7**, 100065.
3 S. Chu, A. L. Wang, A. Bhattacharya and J. K. Montclare, *Prog. Biomed. Eng.*, 2022, **4**, 012003.
4 D. Yi, T. Bayer, C. P. S. Badenhorst, S. Wu, M. Doerr, M. Höhne and U. T. Bornscheuer, *Chem. Soc. Rev.*, 2021, **50**, 8003–8049.
5 A. Z. Haynes and M. Levine, *Anal. Lett.*, 2021, **54**, 1871–1880.
6 Y. Tan, S. Hoon, P. A. Guerette, W. Wei, A. Ghadban, C. Hao, A. Miserez and J. H. Waite, *Nat. Chem. Biol.*, 2015, **11**, 488–495.
7 S. Koga, D. S. Williams, A. W. Perriman and S. Mann, *Nat. Chem.*, 2011, **3**, 720–724.
8 D. G. DeMartini, M. Izumi, A. T. Weaver, E. Pandolfi and D. E. Morse, *J. Biol. Chem.*, 2015, **290**, 15238–15249.
9 K. Hu, J. Morstein and D. Trauner, *Chem. Rev.*, 2018, **118**, 10710–10747.
10 C. P. Carvalho, V. D. Uzunova, J. P. Da Silva, W. M. Nau and U. Pischel, *Chem. Commun.*, 2011, **47**, 8793–8795.
11 T. P. Causgrove and R. B. Dyer, *Chem. Phys.*, 2006, **323**, 2–10.
12 C. Ma, A. Malessa, A. J. Boersma, K. Liu and A. Herrmann, *Adv. Mater.*, 2020, **32**, 1905309.
13 J. Dinic, A. B. Marciel and M. V. Tirrell, *Curr. Opin. Colloid Interface Sci.*, 2021, **54**, 101457.
14 R. Van Der Lee, M. Buljan, B. Lang, R. J. Weatheritt, G. W. Daughdrill, A. K. Dunker, M. Fuxreiter, J. Gough, J. Gsponer, D. T. Jones, P. M. Kim, R. W. Kriwacki, C. J. Oldfield, R. V. Pappu, P. Tompa, V. N. Uversky, P. E. Wright and M. M. Babu, *Chem. Rev.*, 2014, **114**, 6589–6631.
15 W. M. Babinchak and W. K. Surewicz, *J. Mol. Biol.*, 2020, **432**, 1910–1925.
16 E. Rieloff and M. Skepö, *Int. J. Mol. Sci.*, 2021, **22**, 11058.
17 E. Rieloff and M. Skepö, *J. Chem. Theory Comput.*, 2020, **16**, 1924–1935.
18 R. Levenson, C. Bracken, N. Bush and D. E. Morse, *J. Biol. Chem.*, 2016, **291**, 4058–4068.
19 J. Lim, A. Kumar, K. Low, C. S. Verma, Y. Mu, A. Miserez and K. Pervushin, *J. Phys. Chem. B*, 2021, **125**, 6776–6790.
20 R. A. Charafeddine, W. A. Cortopassi, P. Lak, R. Tan, R. J. McKenney, M. P. Jacobson, D. L. Barber and T. Wittmann, *J. Biol. Chem.*, 2019, **294**, 8779–8790.
21 R. Levenson, B. Malady, T. Lee, Y. Al Sabeh, P. Kohl, Y. Li and D. E. Morse, *bioRxiv*, preprint, 2021, DOI: **10.1101/2021.04.23.441158**.
22 J. McCarty, K. T. Delaney, S. P. O. Danielsen, G. H. Fredrickson and J. E. Shea, *J. Phys. Chem. Lett.*, 2019, **10**, 1644–1652.

23 J. W. Bye and R. A. Curtis, *J. Phys. Chem. B*, 2019, **123**, 593–605.
24 S. Lenton, S. Hervø-Hansen, A. M. Popov, M. D. Tully, M. Lund and M. Skepö, *Biomacromolecules*, 2021, **22**, 1532–1544.
25 B. Saha, A. Chatterjee, A. Reja and D. Das, *Chem. Commun.*, 2019, **55**, 14194–14197.
26 I. B. A. Smokers, M. H. I. Van Haren, T. Lu and E. Spruijt, *ChemSystemsChem*, 2022, **4**, e202200004.
27 F. P. Cakmak, S. Choi, M. C. O. Meyer, P. C. Bevilacqua and C. D. Keating, *Nat. Commun.*, 2020, **11**, 5949.
28 S. Jelenic, J. Bindics, P. Czermak, B. R. Pillai, M. Ruer, C. Hoege, A. S. Holehouse and S. Saha, *bioRxiv*, preprint, 2022, DOI: 10.1101/2022.05.16.492059.
29 X. Zhang, Y. Lin, N. A. Eschmann, H. Zhou, J. N. Rauch, I. Hernandez, E. Guzman, K. S. Kosik and S. Han, *PLoS Biol.*, 2017, **15**, e2002183.
30 P. Gracia, D. Polanco, J. Tarancón-Díez, I. Serra, M. Bracci, J. Oroz, D. V. Laurents, I. García and N. Cremades, *Nat. Commun.*, 2022, **13**, 4586.
31 H. Kim, B. jin Jeon, S. Kim, Y. S. Jho and D. S. Hwang, *Polymers*, 2019, **11**, 691–701.
32 E. A. Frankel, P. C. Bevilacqua and C. D. Keating, *Langmuir*, 2016, **32**, 2041–2049.
33 W. M. Babinchak, B. K. Dumm, S. Venus, S. Boyko, A. A. Putnam, E. Jankowsky and W. K. Surewicz, *Nat. Commun.*, 2020, **11**, 5574.
34 D. G. DeMartini, D. V. Krogstad and D. E. Morse, *Proc. Natl. Acad. Sci. U.S.A.*, 2013, **110**, 2552–2556.
35 R. Levenson, C. Bracken, C. Sharma, J. Santos, C. Arata, B. Malady and D. E. Morse, *J. Biol. Chem.*, 2019, **294**, 16804–16815.
36 S. P. Liang, R. Levenson, B. Malady, M. J. Gordon, D. E. Morse and L. Sepunaru, *J. R. Soc. Interface*, 2020, **17**, 20200774.
37 Y. C. Lin, E. Masquelier, Y. Al Sabeh, L. Sepunaru, M. J. Gordon and D. E. Morse, *J. R. Soc. Interface*, 2023, **20**, 20230183.
38 R. Levenson, D. G. DeMartini and D. E. Morse, *APL Mater.*, 2017, **5**, 104801.
39 D. E. Morse and E. Taxon, *Appl. Phys. Lett.*, 2020, **117**, 220501.
40 J. J. Loke, S. Hoon and A. Miserez, *ACS Appl. Mater. Interfaces*, 2022, **14**, 21436–21452.
41 G. Qin, P. B. Dennis, Y. Zhang, X. Hu, J. E. Bressner, Z. Sun, W. J. Crookes-Goodson, R. R. Naik, F. G. Omenetto and D. L. Kaplan, *J. Polym. Sci., Part B: Polym. Phys.*, 2013, **51**, 254–264.
42 E. Kreit, L. M. Mäthger, R. T. Hanlon, P. B. Dennis, R. R. Naik, E. Forsythe and J. Heikenfeld, *J. R. Soc. Interface*, 2013, **10**, 20120601.
43 J. J. Walish, Y. Kang, R. A. Mickiewicz and E. L. Thomas, *Adv. Mater.*, 2009, **21**, 3078–3081.
44 W. Szymański, J. M. Beierle, H. A. V. Kistemaker, W. A. Velema and B. L. Feringa, *Chem. Rev.*, 2013, **113**, 6114–6178.
45 R. J. Mart and R. K. Allemann, *Chem. Commun.*, 2016, **52**, 12262–12277.
46 A. A. Beharry and G. A. Woolley, *Chem. Soc. Rev.*, 2011, **40**, 4422–4437.
47 H. M. D. Bandara and S. C. Burdette, *Chem. Soc. Rev.*, 2012, **41**, 1809–1825.
48 F. A. Jerca, V. V. Jerca and R. Hoogenboom, *Nat. Rev.*, 2022, **6**, 51–69.
49 O. Bozovic, B. Jankovic and P. Hamm, *Nat. Rev. Chem*, 2022, **6**, 112–124.
50 M. Younis, S. Ahmad, A. Atiq, M. A. Farooq, M. H. Huang and M. Abbas, *Chem. Rec.*, 2023, **23**, e202300126.
51 S. Pramanik, B. Kauffmann, S. Hecht, Y. Ferrand and I. Huc, *Chem. Commun.*, 2021, **57**, 93–96.
52 D. Bobrovnikov, M. A. Makurath, C. H. Wolfe, Y. R. Chemla and T. Ha, *J. Am. Chem. Soc.*, 2023, **145**, 21253–21262.
53 D. Leifert, A. S. Moreland, J. Limwongyut, A. A. Mikhailovsky and G. C. Bazan, *Angew. Chem.*, 2020, **59**, 20333–20337.
54 T. Schober, I. Wehl, S. Afonin, O. Babii, A. Iampolska, U. Schepers, I. V. Komarov and A. S. Ulrich, *ChemPhotoChem*, 2019, **3**, 384–391.
55 H. Inaba, M. Sakaguchi, S. Watari, S. Ogawa, A. M. R. Kabir, A. Kakugo, K. Sada and K. Matsuura, *ChemBioChem*, 2023, **24**, e202200782.
56 F. Zhang, O. Sadovski and G. A. Woolley, *ChemBioChem*, 2008, **9**, 2147–2154.
57 D. Moldenhauer, J. P. Fuenzalida Werner, C. A. Strassert and F. Gröhn, *Biomacromolecules*, 2019, **20**, 979–991.
58 I. Willner, M. Lion-Dagan, S. Marx-Tibbon and E. Katz, *J. Am. Chem. Soc.*, 1995, **117**, 6581–6592.
59 S. C. Wang and C. T. Lee, *Biochem.*, 2007, **46**, 14557–14566.
60 P. Mirarefi and C. Ted Lee, *Proteins: Struct., Funct., Bioinf.*, 2019, **87**, 715–722.
61 A. V. Strizhak, O. Babii, S. Afonin, I. Bakanovich, T. Pantelejevs, W. Xu, E. Fowler, R. Eapen, K. Sharma, M. O. Platonov, V. V. Hurmach, L. Itzhaki, M. Hyvönen, A. S. Ulrich, D. R. Spring and I. V. Komarov, *Org. Biomol. Chem.*, 2020, **18**, 5359–5369.
62 I. Wilner, S. Rubin, J. Wonner, F. Effenberger and P. Baeuerle, *J. Am. Chem. Soc.*, 1992, **114**, 3150–3151.
63 T. Shimoboji, Z. L. Ding, P. S. Stayton and A. S. Hoffman, *Bioconjugate Chem.*, 2002, **13**, 915–919.
64 M. Bose, D. Groff, J. Xie, E. Brustad and P. G. Schultz, *J. Am. Chem. Soc.*, 2006, **128**, 388–389.
65 W. Szymański, J. M. Beierle, H. A. V. Kistemaker, W. A. Velema and B. L. Feringa, *Chem. Rev.*, 2013, **113**, 6114–6178.
66 A. Samanta, M. C. A. Stuart and B. J. Ravoo, *J. Am. Chem. Soc.*, 2012, **134**, 19909–19914.
67 Y. H. Liu and Y. Liu, *J. Mater. Chem. B*, 2022, **10**, 958–965.
68 W. Zhan, T. Wei, L. Cao, C. Hu, Y. Qu, Q. Yu and H. Chen, *ACS Appl. Mater. Interfaces*, 2017, **9**, 3505–3513.
69 J. Moratz, A. Samanta, J. Voskuhl, S. K. M. Nalluri and B. J. Ravoo, *Chem.–Eur. J.*, 2015, **21**, 3271–3277.
70 N. Martin, L. Tian, D. Spencer, A. Coutable-Pennarun, J. L. R. Anderson and S. Mann, *Angew. Chem.*, 2019, **131**, 14736–14740.
71 W. Mu, Z. Ji, M. Zhou, J. Wu, Y. Lin and Y. Qiao, *Sci. Adv.*, 2021, **7**, 1–10.

72 Y. Huang, X. Wang, J. Li, Y. Lin, H. Chen, X. Liu and X. Huang, *ChemSystemsChem*, 2021, **3**, e2100006.
73 L. Abate, A. De Robertis and C. Rigano, *J. Solution Chem.*, 1993, **22**, 339–349.
74 J. E. Donald, D. W. Kulp and W. F. DeGrado, *Proteins: Struct., Funct., Bioinf.*, 2011, **79**, 898–915.
75 P. D. Wildes, J. G. Pacifici, G. Irick and D. G. Whitten, *J. Am. Chem. Soc.*, 1971, **93**, 2004–2008.
76 C. Amato, A. Fissi, L. Vaccari, E. Balestreri, O. Pieroni and R. Felicioli, *J. Photochem. Photobiol., B*, 1995, **28**, 71–75.
77 N. Greenfield and G. D. Fasman, *Biochem.*, 1969, **8**, 4108–4116.
78 C. J. Barrow-F, A. Yasuda, P. T. M. Kenny and M. G. Zagorskil, *J. Mol. Biol.*, 1992, **225**, 1075–1093.
79 J. A. Siepen, S. E. Radford and D. R. Westhead, *Protein Sci.*, 2003, **12**, 2348–2359.
80 G. Paramaguru, A. Kathiravan, S. Selvaraj, P. Venuvanalingam and R. Renganathan, *J. Hazard. Mater.*, 2010, **175**, 985–991.
81 P. Bolel, S. Datta, N. Mahapatra and M. Halder, *J. Phys. Chem. B*, 2012, **116**, 10195–10204.
82 A. Adam, S. Mehrparvar and G. Haberhauer, *Beilstein J. Org. Chem.*, 2019, **15**, 1534–1544.
83 C. R. Castor and J. H. Saylor, *J. Am. Chem. Soc.*, 1953, **75**, 1427–1429.